

Original research article

Zebrafish *zic2* controls formation of periorbital neural crest and choroid fissure morphogenesisIrina Sedykh^{a,b,1}, Baul Yoon^{a,b,c,1}, Laura Roberson^{a,b}, Oleg Moskvina^d, Colin N. Dewey^e, Yevgenya Grinblat^{a,b,f,*}^a Department of Integrative Biology, University of Wisconsin, Madison, WI 53706, USA^b Department of Neuroscience, University of Wisconsin, Madison, WI 53706, USA^c Genetics Ph. D. Training Program, University of Wisconsin, Madison, WI 53706, USA^d Primate Research Center, University of Wisconsin-Madison, Madison, WI 53706, USA^e Department of Biostatistics and Medical Informatics, University of Wisconsin-Madison, Madison, WI 53706, USA^f McPherson Eye Research Institute, University of Wisconsin, Madison, WI, 53706, USA

ARTICLE INFO

Keywords:

Zic2

Alx1

Hedgehog signaling

Coloboma

Zebrafish

ABSTRACT

The vertebrate retina develops in close proximity to the forebrain and neural crest-derived cartilages of the face and jaw. Coloboma, a congenital eye malformation, is associated with aberrant forebrain development (holoprosencephaly) and with craniofacial defects (frontonasal dysplasia) in humans, suggesting a critical role for cross-lineage interactions during retinal morphogenesis. ZIC2, a zinc-finger transcription factor, is linked to human holoprosencephaly. We have previously used morpholino assays to show zebrafish *zic2* functions in the developing forebrain, retina and craniofacial cartilage. We now report that zebrafish with genetic lesions in zebrafish *zic2* orthologs, *zic2a* and *zic2b*, develop with retinal coloboma and craniofacial anomalies. We demonstrate a requirement for *zic2* in restricting *pax2a* expression and show evidence that *zic2* function limits Hh signaling. RNA-seq transcriptome analysis identified an early requirement for *zic2* in periorbital neural crest as an activator of *alx1*, a transcription factor with essential roles in craniofacial and ocular morphogenesis in human and zebrafish. Collectively, these data establish *zic2* mutant zebrafish as a powerful new genetic model for in-depth dissection of cell interactions and genetic controls during craniofacial complex development.

1. Introduction

The key portion of the vertebrate eye, the neural retina, begins its development as an integral part of the forebrain primordium. It evaginates to form bilateral optic vesicles that connect to the forebrain via the optic stalks (OS). Optic vesicles then fold into cup-like structures that briefly remain open at the site adjacent to OS, termed the choroid fissure (Bazin-Lopez et al., 2015; Gestri et al., 2012; Kwan, 2014; Schmitt and Dowling, 1994). The edges of the choroid fissure come together and fuse during normal development; failure of this process results in uveal coloboma, estimated to occur once in every 5000 births (Williamson and FitzPatrick, 2014). Coloboma is a significant cause of congenital blindness, found in 3–11% of blind children (Onwoche et al., 2000). Despite its prevalence and debilitating consequences, the underlying molecular defects that cause coloboma are not well understood.

The choroid fissure forms in a complex environment that includes the adjacent forebrain and neural crest (NC)-derived mesenchymal

cells on their way to becoming skeletal and vascular elements of the face and jaw. In zebrafish, NC cells that migrate in the anterior streams around the optic vesicle form the neurocranium (ethmoid plate and the trabeculae) (Schilling et al., 1999; Wada et al., 2005). The retina and OS signal to the anterior NC, directing it to its destinations (Eberhart et al., 2008; Kish et al., 2011; Swartz et al., 2011). There is emerging evidence for a reciprocal interaction, whereby NC cells signal back to the eye and brain (reviewed in Bazin-Lopez et al. (2015), Gestri et al. (2012), Le Douarin et al. (2007)). In humans, significant comorbidity has been reported between frontonasal dysplasia and coloboma (Wu et al., 2007), suggesting that NC plays a specific role in choroid fissure morphogenesis. The importance of this mechanism has only recently come to light and needs robust genetic models to be fully understood.

Dysregulation in several signaling pathways has been implicated in coloboma, with Hedgehog (Hh) signaling arguably the best characterized (Williamson and FitzPatrick, 2014). Disruption of Hh signaling also causes forebrain anomalies called holoprosencephaly (HPE)

* Corresponding author.

E-mail address: ygrinblat@wisc.edu (Y. Grinblat).¹ These authors contributed equally to the work.

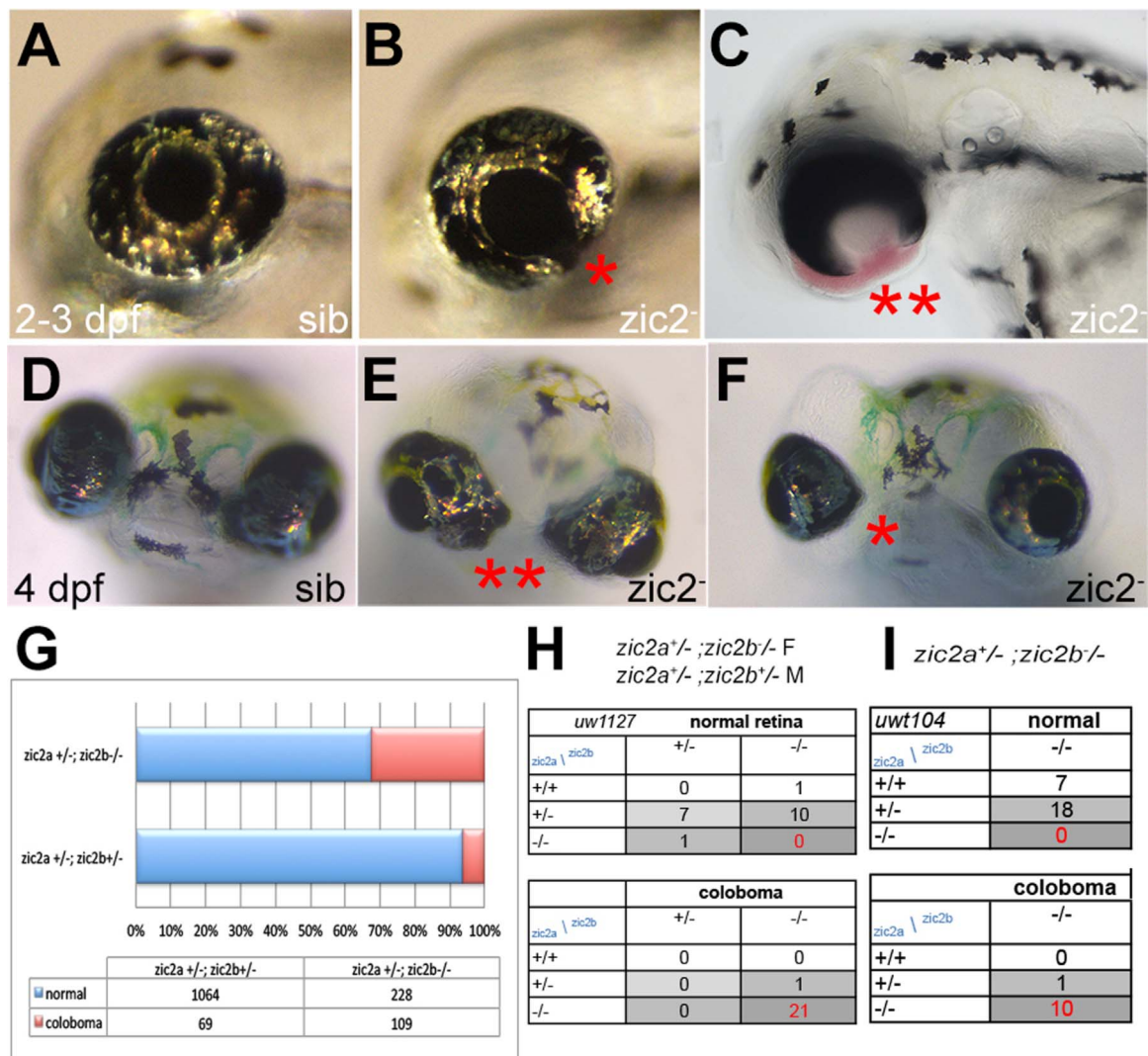


Fig. 1. Zebrafish *Zic2* is required during retinal morphogenesis. A: normal retinal morphology. B: retina exhibiting mild coloboma (*). C: retina exhibiting severe coloboma with periocular hemorrhaging (**). D: normal retinal morphology. E: bilateral coloboma in a severely affected embryo (**). F: mild, unilateral coloboma in an affected embryo. G: Penetrance and expressivity of coloboma is increased in progeny that lack maternal *zic2b*, derived from *zic2a*^{gbl133}/+; *zic2b*^{t104}/zic2b^{t104} parents, compared to those from double heterozygous (*zic2a*^{gbl133}/+; *zic2b*^{t104}/+) parents (see Table S1 for details). H, I: Both CRISPR- and TALEN-induced mutant alleles of *zic2b* are tightly associated with coloboma in MZ-*zic2* embryos. Embryos in A-C are at 2–3 dpf, shown in lateral views, anterior to the left. Embryos in D-F are at 4 dpf, shown in anterior views, dorsal at the top.

(Roessler et al., 1996; Roessler and Muenke, 2010), and facial dysmorphologies that range from hypertelorism (increased distance between eye orbits) attributed to increased Hh signaling to orofacial clefting caused by Hh reduction (Brugmann et al., 2010; Gongal et al., 2011; Young et al., 2010). To understand how Hh signaling controls these processes, it is necessary to examine the downstream effectors of Hh signaling in each developmental context.

zic2, a member of the conserved *Zic* family of zinc-finger transcription factors, is one such effector. *zic2* plays a key role in brain morphogenesis, as indicated by the high incidence of *zic2* mutations in human patients with HPE (Brown et al., 2001, 1998; Ribeiro et al., 2012; Roessler et al., 2009; Solomon et al., 2010). Extensive studies in mouse and *Xenopus* have demonstrated essential roles for *zic2* in early neural development, namely, neural crest specification and neural tube closure (Elms et al., 2004, 2003; Houtmeyers et al., 2016; Nagai et al., 2000, 1997; Nakata et al., 1997, 1998; Nyholm et al., 2009; Teslaa et al., 2013; Warr et al., 2008; Ybot-Gonzalez et al., 2007). *Zic2* is also required for specification of embryonic stem cells, where it functions as an enhancer-binding cofactor in concert with the Mbd3-NuRD chromatin remodeling complex (Luo et al., 2015). Later in development, *zic2* function is required for correct migration of cortical neurons

(Murillo et al., 2015), for cerebellar granular neuron differentiation (Frank et al., 2015) and as a key determinant of ipsilateral vs contralateral projection in retinal ganglion cells (Escalante et al., 2013; Garcia-Frigola et al., 2008; Herrera et al., 2003). In hypomorphic *zic2* mice, defective retinal morphogenesis has been reported, but not characterized (Herrera et al., 2003). The underlying mechanism of its functions during development have been elusive until recently, when *zic2* was found to inhibit canonical Wnt signaling (Fujimi et al., 2012; Pourebrahim et al., 2011), and to control forebrain morphogenesis via a direct interaction with Smad2/3 in the Nodal signal transduction pathway (Houtmeyers et al., 2016). To fully understand the mechanism of *zic2* functions in the context of the developing embryo, it is essential that we dissect these functions further, and in more than one model organism.

Here we report that zebrafish with genetic lesions in zebrafish *zic2* orthologs, *zic2a* and *zic2b*, develop with profound retinal and craniofacial anomalies, similar to those observed after transient depletion of *zic2* by antisense morpholino oligos (Sanek et al., 2009; Teslaa et al., 2013). We show that *zic2* function is required for the correct morphogenesis of the OS and for juxtaposing the edges of the fissure to allow its subsequent closure. We demonstrate a requirement for *zic2*

in restricting *pax2a* expression at the OS/ventral retina border, and show evidence of increased Hh signaling in the absence of *zic2* function. Using RNA-seq-based transcriptome analysis, we confirm an early requirement for *zic2* function in NC-derived pharyngeal and periocular neural crest, and identify a novel role for *zic2* as a transcriptional activator of *Alx1*, a paired homeobox transcription factor with key functions in craniofacial and ocular morphogenesis in human and zebrafish embryos (Dee et al., 2013; Uz et al., 2010). Collectively, these data establish *zic2* mutant zebrafish as a powerful new genetic model for in-depth dissection of the complex inter-lineage cell interactions and genetic controls during craniofacial complex development.

2. Results

2.1. Zebrafish *zic2* orthologs function redundantly during retinal and craniofacial morphogenesis

Zebrafish *zic2* orthologs *zic2a* and *zic2b*, the only members of the *Zic* gene family duplicated in teleosts, reside on chromosomes 9 and 1, respectively. To build a genetic model of *zic2*-linked HPE in zebrafish, we set out to establish lines mutant at both loci. Toward this end, we obtained a mutagenic gene-trap insertion in the first coding exon of *zic2a*, *zic2a*^{gbt133}, isolated in a screen by Clark et al. (2011) (Fig. S1). *zic2a*^{gbt133} homozygous embryos develop normally for the first 2 weeks (data not shown), likely due to functional redundancy with its ortholog, *zic2b*. We used targeted mutagenesis with TALEN and CRISPR/Cas9 to generate frame-shift alleles at two distinct sites in the first exon of the *zic2b* locus (see Section 4 for details). Three mutant alleles were isolated that contained a 27-nt insertion (*zic2b*¹¹²⁷) or a 16-nt insertion (*zic2b*¹¹¹⁶) at the CRISPR target site, and a 4-nt deletion (*zic2b*¹¹⁰⁴) at the TALEN target site (Fig. S1). *zic2b* homozygous mutants developed normally and were viable as adults despite the predicted absence of full-length *zic2b* protein; in contrast, ~ 5% of the embryos derived from a double heterozygous (*zic2a*^{+/−}; *zic2b*^{+/−}) incross exhibited retinal coloboma by 48 hpf (Fig. 1A–F; Table S1). The expected proportion of *zic2a*; *zic2b* homozygous mutants (*zic2* mutants) is 6.25%. Affected embryos frequently presented with mild coloboma, defined here as a relatively small gap present in only one of the two retinæ (Fig. 1B, G). Unexpectedly, a subset of embryos with coloboma exhibited periocular hemorrhage and edema, indicative of vascular deficits (Fig. 1C, F).

We next asked if the maternal function of *zic2* played a role during retinal development by assessing embryonic phenotypes in progeny from a cross between *zic2a*^{+/−}; *zic2b*^{−/−} parents, 25% of which are predicted to be *zic2* mutants. 25% of these embryos exhibited coloboma by 2 dpf (Table S1); coloboma was primarily severe, i.e. bilateral with large ventral gaps (Fig. 1C, E, G), consistent with a requirement for maternal *zic2b* during retinal morphogenesis. To confirm that *zic2* mutations were responsible for abnormal retinal morphogenesis, we genotyped representative embryos with and without coloboma individually (Fig. S2). This analysis showed that the majority of embryos with coloboma were *zic2* mutants (going forward, we will refer to *zic2* mutants derived from *zic2b*^{−/−} mothers as MZ-*zic2* mutants). Coloboma was also occasionally observed in maternally depleted embryos with one wildtype allele of *zic2a* (Fig. 1H, I).

By 5 dpf, all embryos with coloboma exhibited profoundly hypoplastic craniofacial cartilages, both in the neurocranium and pharyngeal arches, and severe periocular and cranial edema (Fig. 2A, B; Table S2). Similar defects were observed in embryos produced by heterozygous parents and those from *zic2a*^{+/−}; *zic2b*^{−/−} parents (data not shown). Genotypic analysis revealed that this phenotype was restricted to *zic2* mutants and embryos with one wildtype allele of *zic2a* (Fig. 2C,D). Collectively, these data clearly demonstrate a requirement for zygotic *zic2* function in the developing retina and craniofacial cartilages, and an early contribution of maternal *zic2b* function to retinal morphogenesis.

2.2. *zic2* restricts expression of *pax2a* in the optic stalk

We next asked if ventral retinal patterning and/or morphology were disrupted in *zic2* mutants at 24 hpf, prior to the first appearance of overt coloboma. The choroid fissure and the OS are marked by patterned expression of several homeobox transcription factors, including *pax2a* (Macdonald et al., 1995; Mui et al., 2005; Takeuchi et al., 2003). We examined *pax2a* expression in *zic2* embryos using whole mount in situ hybridization (WISH). Embryos derived from *zic2a*^{+/−}; *zic2b*^{+/−} parents exhibited normal expression of *pax2a* overall with the exception of the OS domain, which was mispatterned in 12% of the embryos (Fig. 3A, B). Post-hoc genotyping confirmed that all the embryos with mispatterned *pax2a* were homozygous for *zic2b* (Fig. 3C). All embryos with mispatterned *pax2a* exhibited aberrant ventral retina (Fig. 3D–F), i.e. were also *zic2a*^{gbt133} homozygous. We next applied confocal microscopy to examine distribution of the Pax2a epitope in 24 hpf MZ-*zic2* mutants. Normal retina expressed Pax2a in the restricted portion of the retina adjacent to the choroid fissure (Fig. 3G). In MZ-*zic2* mutants, retinal edges of the choroid fissure expressed Pax2a, but were separated by a large gap. The OS were abnormally wide and contained aberrantly high *pax2a* signal (Fig. 3H). We also noted an intense concentration of F-actin at the choroid fissure in normal siblings and an absence thereof in mutant retina, consistent with aberrant morphogenesis. These observations are consistent with our previous finding that *pax2a* is ectopically expressed in embryos transiently depleted of *zic2a* (Sanek et al., 2009). When examined in ventral cross-sections, MZ-*zic2* mutants exhibited aberrant expansion of Pax2a both in the ventral retina and in the pre-optic diencephalon contiguous with the OS (Fig. 3I, J). Pax2a-expressing diencephalon appeared dysmorphic, with thinner walls and larger lumen than the equivalent structure in the unaffected siblings (Fig. 3K, L). Collectively, these observations indicate an early requirement for *zic2* function during morphogenesis of both the OS/choroid fissure boundary and the adjacent diencephalon.

Hedgehog growth factors secreted from the ventral diencephalic midline pattern the OS and retina, partitioning it into three domains: the OS, ventral retina and dorsal retina (Ekker et al., 1995; Lee et al., 2008a; Lupo et al., 2005; Schimmenti et al., 2003; Varga et al., 2001; Wang et al., 2015). Since *pax2a* requires Hh signaling for its expression, *pax2a* expansion in *zic2* mutants may indicate aberrant levels of Hh or an aberrant downstream transcriptional response. Zebrafish that lack the functional Hh receptor *blowout/ptc1* due to mutations show increased levels Hh signaling and develop with incompletely penetrant coloboma; this defect is efficiently rescued by exposure to low levels of cyclopamine, a small molecule that inhibits Hh signaling (Lee et al., 2008a). Cyclopamine treatment also rescues coloboma caused by knockdown of *sox4* or *sox11*, transcription factors that function as inhibitory modulators of Hh signaling during retinal morphogenesis (Pillai-Kastoori et al., 2014; Wen et al., 2015). We reasoned that, if Hh signaling is expanded in *zic2* mutants, inhibition of Hh signaling should reduce the penetrance and/or expressivity of coloboma. To test this prediction, we exposed progeny from *zic2a*^{+/−}; *zic2b*^{−/−} incrosses to low concentration of cyclopamine that was sufficient to rescue coloboma in *blowout/ptc1* mutants (Lee et al., 2008a). When progeny from *zic2a*^{+/−}; *zic2b*¹¹⁰⁴ parents were exposed to cyclopamine during gastrulation and somitogenesis, they developed with significantly milder coloboma than their vehicle-treated siblings (Fisher Exact test, $p < 0.02$, Fig. 4A–E, Fig. S3). The overall morphology of the embryos was not affected at this cyclopamine concentration (3–4.5 μ M). To test specificity of the rescue, we asked if cyclopamine rescue is allele-independent. Progeny from *zic2a*^{+/−}; *zic2b*^{uw1116} parents exhibited significant alleviation of coloboma phenotype after cyclopamine treatment (Fisher Exact test, $p < 0.04$; Fig. 4E, Fig. S3). In contrast, cyclopamine did not significantly affect coloboma penetrance or expressivity in zygotic *zic2* mutants (Fig. 4F, Fig. S3). These findings are consistent with the notion that Hh signaling is de-repressed in the

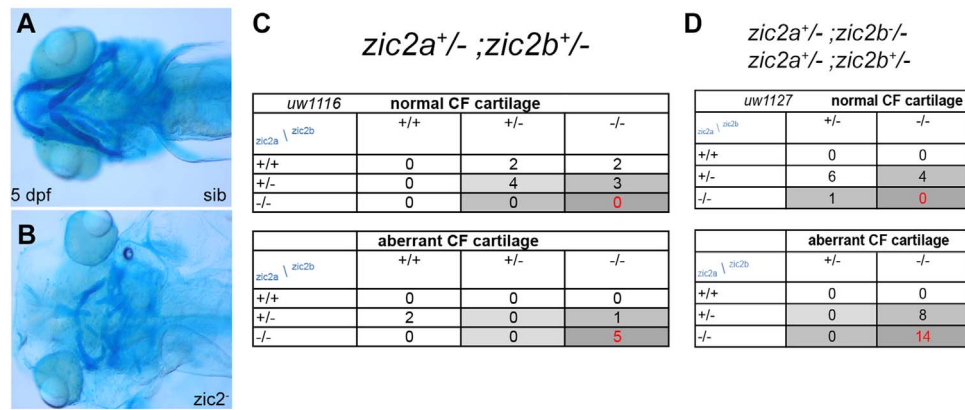


Fig. 2. Zebrafish *Zic2* is required for craniofacial cartilage development. **A:** normal neurocranium and branchial arches. **B:** hypoplastic, disorganized craniofacial cartilages in a *zic2* mutant. **C:** Craniofacial defects are enriched in *zic2* mutants derived from double heterozygous parents. **D:** In embryos that lack maternal *zic2b*, craniofacial defects are observed in *zic2* mutants and in embryos with one wildtype copy of *zic2a*. Cartilage was visualized by staining with Alcian Blue. Embryos at 5 dpf are shown in ventral views, anterior to the left.

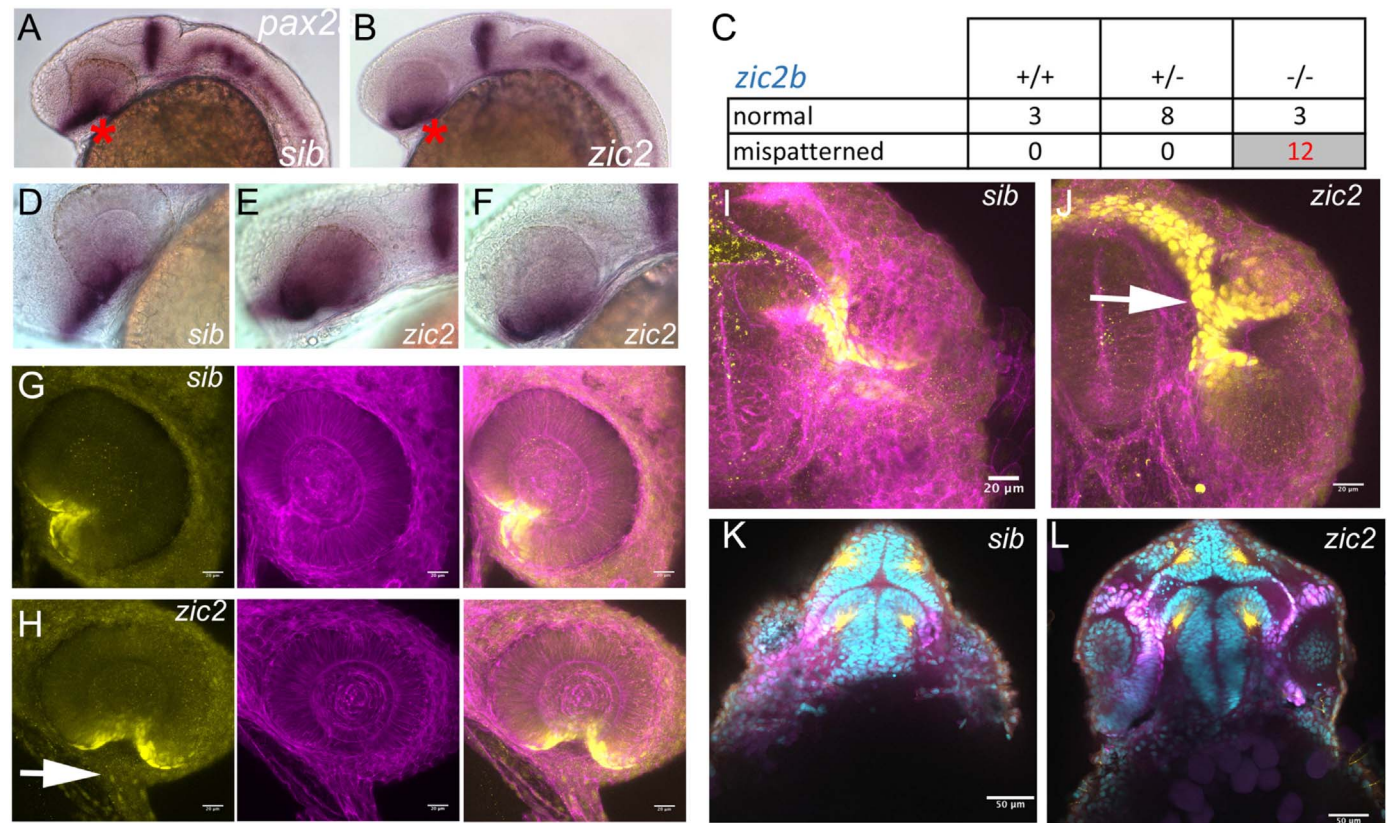


Fig. 3. *Pax2a* expression is aberrant in MZ-*zic2* mutants at 1 dpf. *pax2a* expression at 1 dpf was visualized in embryos derived from $zic2a^{gbt133}/+; zic2b^{uw1116}/+$ parents using WISH (A–F) or in progeny of $zic2a^{gbt133}/+; zic2b^{uw1104}$ parents using immunohistochemistry (G–L). **A:** normal *pax2a* expression in the ventral retina (*). **B:** mispatterned *pax2a* expression (*) was observed in 12 out of 103 embryos (12%, 2 expts.). **C:** Only *zic2b* homozygous embryos exhibit *pax2a* mispatterning. *zic2a* genotype was not tested because PCR genotyping was not robust after WISH. **D–F:** Embryos with mispatterned *pax2a* expression also exhibit coloboma, indicative of homozygosity for *zic2a^{gbt133}*. **G, H:** confocal stacks through representative retina of normal (G) and *zic2* mutant (H) retina. **I, J:** confocal stacks through the ventral aspects of a normal (I) and *zic2* mutant (J) diencephalon and retina. Arrowheads in H, J point to the aberrant optic stalk. In G–J, yellow = *Pax2a*, magenta = F-actin cytoskeleton visualized by phalloidin. **K, L:** single confocal sections through representative normal (K) and *zic2* mutant (L) embryos, imaged ventrally at the level of choroid fissure. magenta = *Pax2a*; yellow = acetylated tubulin; cyan = nuclei visualized by DAPI. Embryos are shown in lateral views, anterior to the left (A–F) or anterior to the right (G, H); in ventral views with anterior at the top (I–L).

absence of functional *zic2* and that this de-repression contributes to retinal dysmorphology in *zic2* mutants.

2.3. *Zic2* function is required for neural crest-derived craniofacial lineage formation

We next set out to identify downstream effectors of *zic2*, i.e. genes whose transcription levels depend on *zic2* function, using RNA-seq transcriptomic analysis (Fig. 5A). Embryos derived from $zic2a^{+/-}; zic2b$

$+/-$ parents were sorted by coloboma at 25–28 hpf, when coloboma first manifests in *zic2* mutants. RNA was isolated from individual embryos without pooling to increase the statistical power of analysis and subjected to high-throughput sequencing (see Section 4 for details). RNA-seq was performed on 10 samples in total, 5 normal and 5 with coloboma. One of the wild type samples was determined to be a mutant and excluded from further analysis. This approach identified a large set of 362 genes differentially expressed in *zic2* mutants (199 increased and 169 reduced) (Table S3). We used the online bioinformatics tool (Huang et al., 2009)

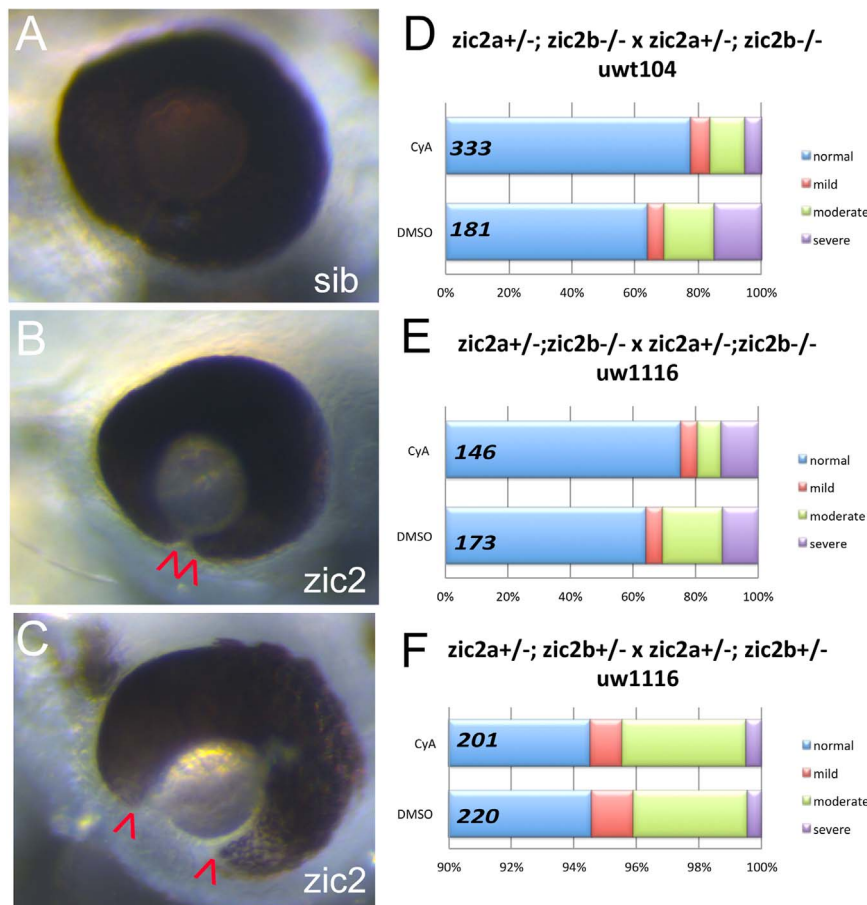


Fig. 4. Cyclopamine treatment reduces frequency and severity of coloboma in *zic2* mutants. A: normal retinal morphology; B: retina with mild coloboma; C: retina with moderate coloboma. D: Embryos were derived from *zic2a*^{gbl133}/⁺; *zic2b*^{u1104} parental crosses and exposed to 3 or 4.5 μ M cyclopamine (CyA) from 3 to 5 hpf until 24–26 hpf. In CyA-treated groups (3 expts; Fig. S3A), the proportion of embryos with coloboma was reduced significantly compared to vehicle-treated control siblings (Fisher's Exact test, $P < 0.001$). Proportion of severely affected embryos among all embryos with coloboma was also decreased in CyA-treated siblings (Fisher's Exact test, $p < 0.02$). E: Embryos were derived from *zic2a*^{gbl133}/⁺; *zic2b*^{uw1116} parents, and treated starting at 3 hpf with 4.5 μ M CyA. CyA-treated groups exhibited reduction in coloboma penetrance (Fisher's Exact test $p < 0.04$) compared to vehicle-treated control siblings (2 expts; Fig. S3B). F: Embryos were derived from *zic2a*^{gbl133}/⁺; *zic2b*^{uw1116}/⁺ parents, and treated as in D with 4.5 μ M CyA or vehicle starting at 3 hpf. Proportion of embryos with coloboma was not affected by exposure to cyclopamine (2 expts). Embryos with unilateral mild coloboma were scored as "mild"; embryos with bilateral mild coloboma were scored as "moderate", and embryos with bilateral moderate coloboma were scored as "severe".

to sort the responsive gene list into categories based on tissue enrichment in zebrafish (ZFIN_ANATOMY). This analysis identified myotome/somite, craniofacial elements, and heart (enrichment scores 2.78, 2.24 and 1.71, respectively). Myotome/somite markers and heart markers were found primarily in the upregulated set, consistent with expression of *zic2b* in zebrafish somites (Toyama et al., 2004) and with the demonstrated function for mammalian *Zic2* during myogenesis (Inoue et al., 2007; Pan et al., 2011). In contrast, craniofacial markers appeared among transcripts depleted in *zic2* mutants (Fig. 5A). This set included chondrogenic neural crest markers *dlx1a*, *dlx2a*, *dlx4a* and *barx1*, and xanthophore lineage markers *aox5*, *gch2* and *cax1* (references in Table S4). We have previously shown both lineages to be strongly dependent on *zic2* function in morpholino assays (Teslaa et al., 2013). A small number of retinal markers were also reduced in *zic2* mutants, namely, *vax1* and *vax2*, Hh-regulated OS/ventral retina markers (Takeuchi et al., 2003), and *atoh7*, expressed in retinal ganglion cells (Masai et al., 2000). Notably, *pax2a* transcript levels were unchanged in *zic2* mutants, perhaps because the mispatterning we have documented in Fig. 3 affects a small portion of its expression domain.

To validate these results, we used WISH on *zic2* mutants and siblings. *Dllx2a* was specifically reduced in pharyngeal arch primordia at 24 hpf, but not in the tel- or diencephalon, in 6% of progeny from *zic2a*^{+/−}/*zic2b*^{+/−} parents (Fig. 5B–E), and this reduction was restricted to *zic2b*^{−/−} embryos (Fig. 5F). Reduced expression of *atoh7* and *vax2* was also confirmed by WISH (Fig. S4).

Cldn11a, a tight junction component enriched in myelinating oligodendrocytes (Bronstein et al., 1997; Morita et al., 1999) was the most strongly depleted gene identified by RNA-seq (Fig. 5A). In zebrafish, *cldn11a* expression has been reported in vascular endothelium (Cannon et al., 2013). In contrast, we found *cldn11a* expression to be restricted to a small group of cells anterior to the retina, in close proximity to the choroid fissure, at 24 hpf (Fig. 5G). Consistent with RNA-seq results, *cldn11a* expression was nearly abolished in *zic2* mutants assayed by WISH (Fig. 5H). Notably, *cldn11* transcription requires *zic2* function in the differentiating mammalian cerebellar ganglion cells (Frank et al., 2015).

2.4. *Zic2* controls transcription of *alx1* in the periocular neural crest

One of the candidate targets of *zic2* identified by RNA-seq, *Alx1*, is expressed in chondrogenic neural crest and functions during retinal and craniofacial cartilage morphogenesis. Homozygous mutations in *alx1* are associated with profound frontonasal dysplasia and microphthalmia in humans (Bertola et al., 2013; Uz et al., 2010), and zebrafish *alx1* morphants develop with hypoplastic craniofacial cartilages and coloboma (Dee et al., 2013). WISH analysis corroborated depletion of *alx1* transcript in *zic2* mutants (Fig. 6A,B). We examined expression of *alx1* during normal development to verify its restriction to neural crest. At 16 hpf, *alx1* was expressed in the frontonasal neural crest, which forms the facial skeleton (Couly et al., 2002; Langenberg

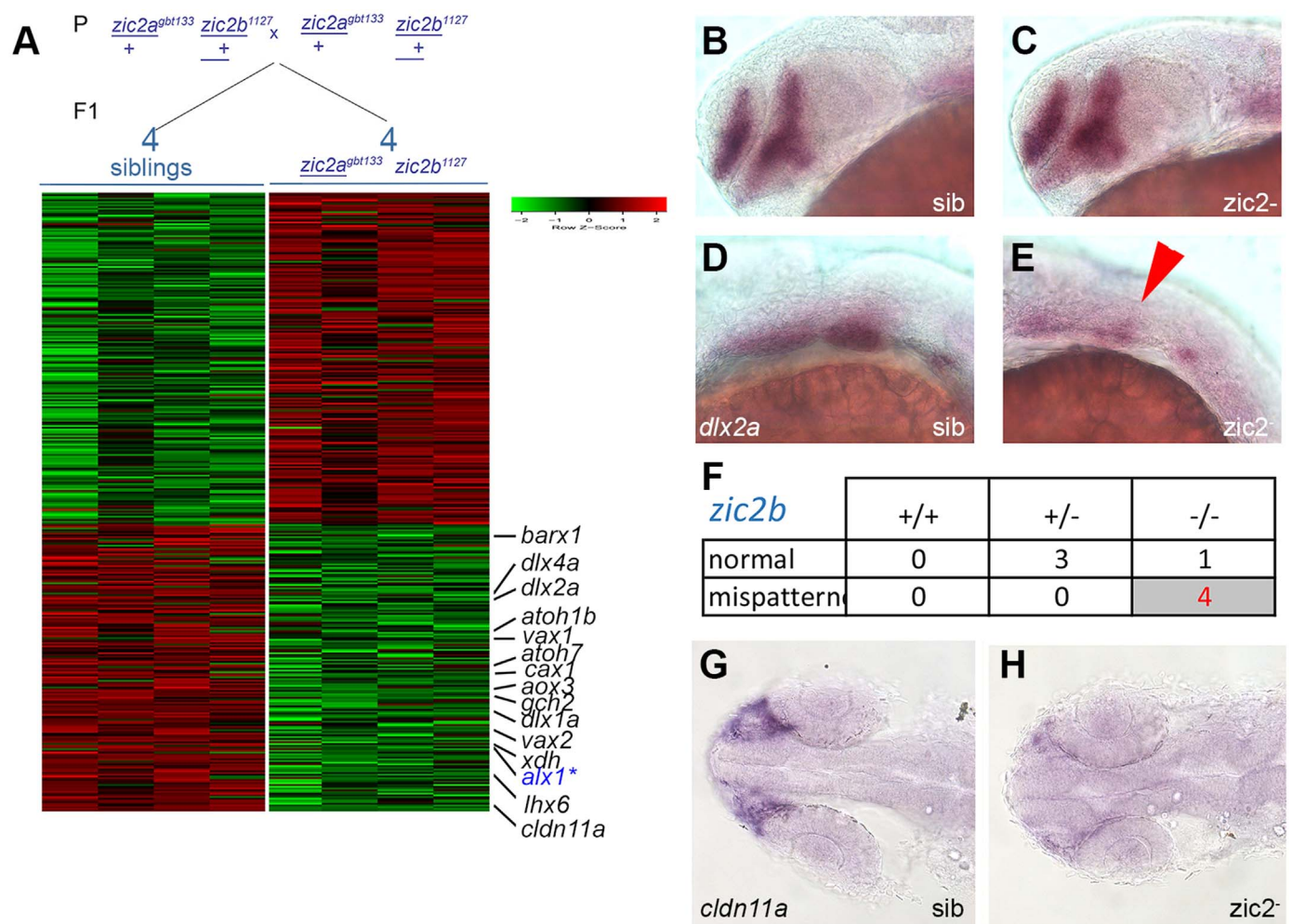


Fig. 5. RNA sequencing transcriptome analysis identifies a set of *Zic2*-dependent targets. **A:** Embryos derived from $zic2a^{gbt133}/+; zic2b^{1127}/+$ parents were sorted by presence or absence of coloboma into *zic2* mutants and sibling groups, respectively. RNA extracted from individual embryos (4 wildtype and 5 with coloboma) was used to prepare cDNA libraries for illumina high-throughput sequencing. Genes with assigned value of False-Discovery Rate below 0.05 were preliminarily selected. The heat-map color represents relative expression levels of differentially expressed genes; 4 out of 5 coloboma-representing libraries are shown to maintain visual balance with the 4 normal sibling samples. **B, C:** Representative sibling and *zic2* mutant embryos derived from $zic2a^{gbt133}/+; zic2b^{1127}/+$ parents show normal *dlx2a* expression by WISH in the telencephalon and diencephalon. **D:** normal *dlx2a* expression in branchial arch primordia. **E:** depleted branchial arch *dlx2a* expression (arrowhead) was observed in 7 out of 127 (6%, 3 expts.) of embryos from this cross. **F:** Only *zic2b*^{-/-} homozygotes exhibited *dlx2a* reduction in branchial arch primordia. **G:** normal *cldn11a* expression adjacent to the optic stalk of embryo with normal retinal morphology. **H:** depleted *cldn11a* expression in *zic2* mutant with coloboma. Embryos in **B – E** are shown in lateral views, anterior to the left. Embryos in **G** and **H** are shown in dorsal views, anterior to the left.

et al., 2008) (Fig. 6C, D). *alx1* was expressed in the periocular region at 24 and 36 hpf (Fig. 6E, F) and in the ethmoid plate anlagen at 48 hpf (Fig. 6F). *alx1* was also expressed in the prospective swim bladder, but this domain did not appear to be affected in *zic2* mutants (not shown).

To ask if *alx1* depletion was indicative of a broader periocular mesenchyme deficit, we examined expression of *crestin*, an early general marker of neural crest (Langenberg et al., 2008) in MZ-*zic2* mutants and siblings. We found the anterior stream of *crestin*-positive neural crest and its pharyngeal domain strongly reduced in *zic2* mutants (Fig. 7A–E). In contrast, *crestin*-expressing cells in the trunk appeared unaffected (Fig. 7C, F).

Since *crestin* is not expressed in the ventral portion of periocular neural crest, we examined this NC population directly by high-resolution confocal imaging. MZ-*zic2* mutants and their siblings were fixed at 24 hpf and stained for F-actin and DNA to visualize cell outlines and nuclei. In normal siblings, cells with mesenchymal appearance were observed in the periocular space adjacent to the choroid fissure; these were enriched in the proximal (closest to the OS) half of the optic cup (Fig. 8A–C). In contrast, the ventral periocular space was largely devoid of cells along the entire proximodistal axis of the mutant optic cup (Fig. 8D–F). Taken together, these data argue that *zic2* plays a critical early role during periocular neural crest formation.

3. Discussion

The data presented here establish the first genetic model of *zic*-linked birth defects in zebrafish and extends our understanding of how *zic2* coordinates development of the craniofacial complex comprised of brain, retina and craniofacial cartilages. We show that zebrafish *zic2a* and *zic2b* function redundantly to promote Hh-dependent retinal morphogenesis, and demonstrate a requirement for both zygotic and maternal *zic2* in controlling morphogenesis of the optic stalk and retina, and to restrict *pax2a* expression in this region. This study confirms a key early role for *zic2* in neural crest formation and identifies a homeobox transcription factor *Alx1* as a novel effector of *zic2* function in the periocular neural crest.

3.1. Where does *zic2* function to control eye morphogenesis?

Our transcriptome analysis identified an early requirement for *zic2* function in a number of neural crest lineages, particularly in the cartilage precursors of the branchial arches and in periocular neural crest. Zebrafish *zic2a* and *zic2b* are predominantly expressed in the presumptive neural crest (Grinblat and Sive, 2001; Nyholm et al., 2007; Teslaa et al., 2013; Toyama et al., 2004); hence it is tempting to

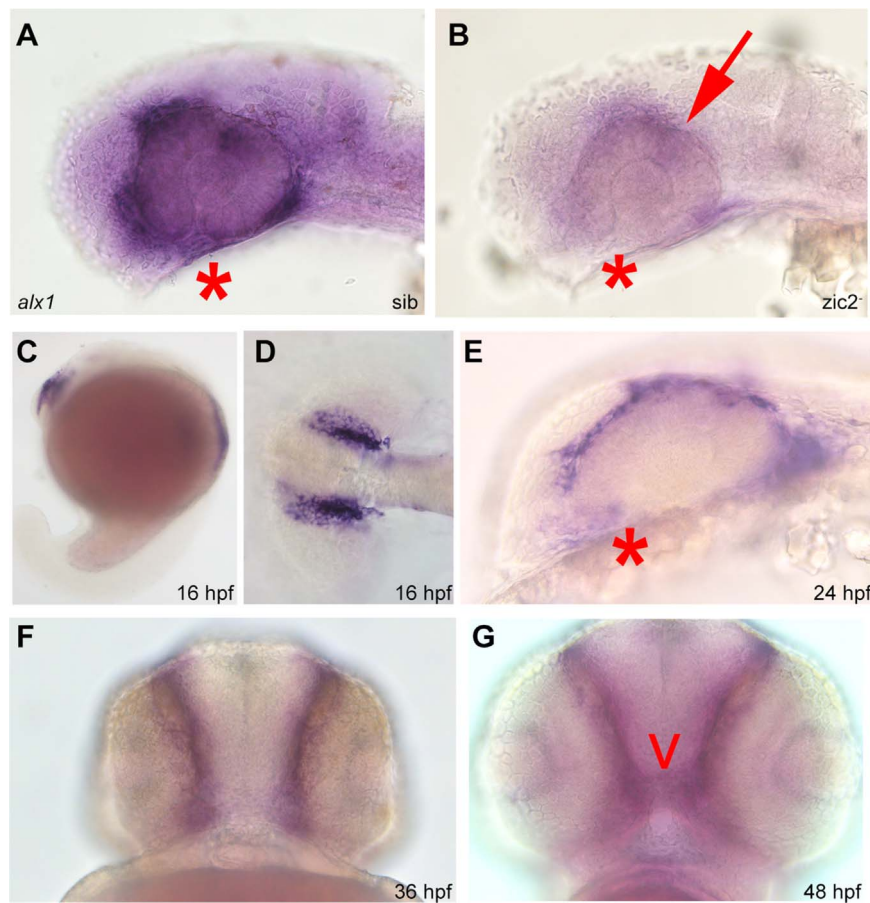


Fig. 6. Alx1 is a novel target of zic2 in the periocular neural crest. Embryos derived from *zic2a*^{gbt133}/+; *zic2b*^{t104}/*zic2b*^{t104} parents were stained for alx1 expression by WISH. A: normal expression in periocular mesenchyme of sibling embryo. B: depleted expression in zic2 (arrow) in mutant embryo (39 out of 112 total, 2 expts). C-G: wild type embryos stained for alx1 expression by WISH. C-D: alx1 is expressed in frontonasal neural crest at 16 hpf. E, F: alx1 is expressed in periocular mesenchyme (*) at 24 hpf and 36 hpf. G: alx1 is expressed in the ethmoid plate (arrowhead) at 48 hpf. Embryos in A, B, C, and E are shown in lateral views, anterior to the left. Embryo in D is shown dorsally, anterior to the left. Embryos in F and G are shown in anterior views, ventral at the top.

speculate that *zic2* controls ventral retinal morphogenesis indirectly, via a primary function in neural crest. Alx1 is an attractive candidate effector of Zic2, since *alx* gene family members function in periocular neural crest to regulate retinal morphogenesis in human, mouse and

zebrafish (Bertola et al., 2013; Dee et al., 2013; Lakhwani et al., 2010; Qu et al., 1999; Uz et al., 2010; Zhao et al., 1996).

Non-cell-autonomous roles for periocular neural crest in choroid fissure morphogenesis have been demonstrated in mouse mutants

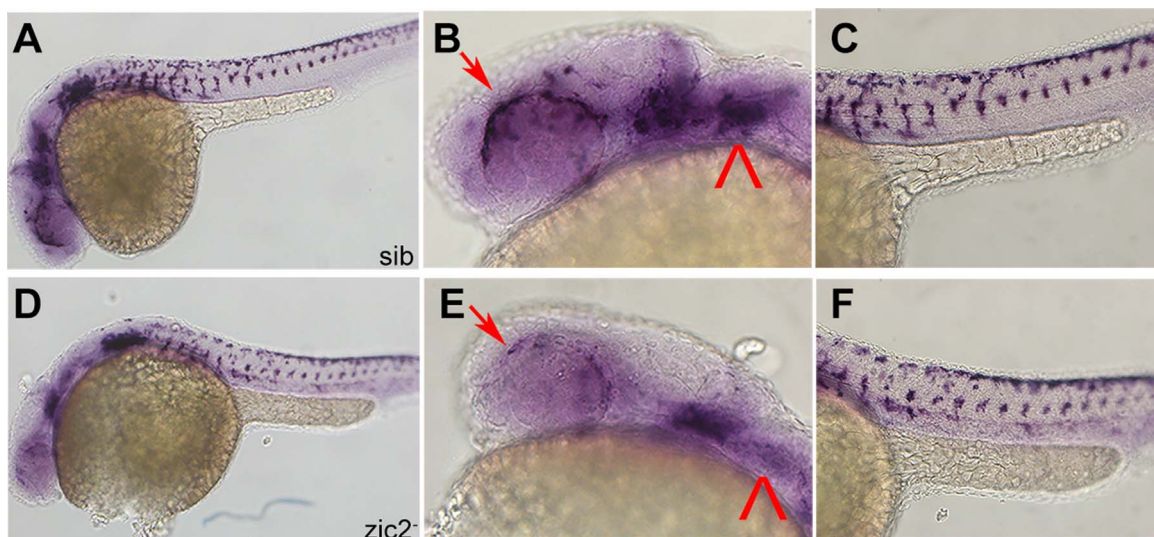


Fig. 7. Frontonasal and pharyngeal neural crest is depleted in MZ-*zic2* mutants. A-C: normal crestin expression in frontonasal and pharyngeal neural crest. D-F: depleted crestin expression in 14 of 55 embryos from a *zic2a*^{gbt133}/+; *zic2b*^{t104}/*zic2b*^{t104} incross. Arrows point to periocular neural crest. Arrowhead points to pharyngeal arch expression. Embryos are shown in lateral views, anterior to the left.

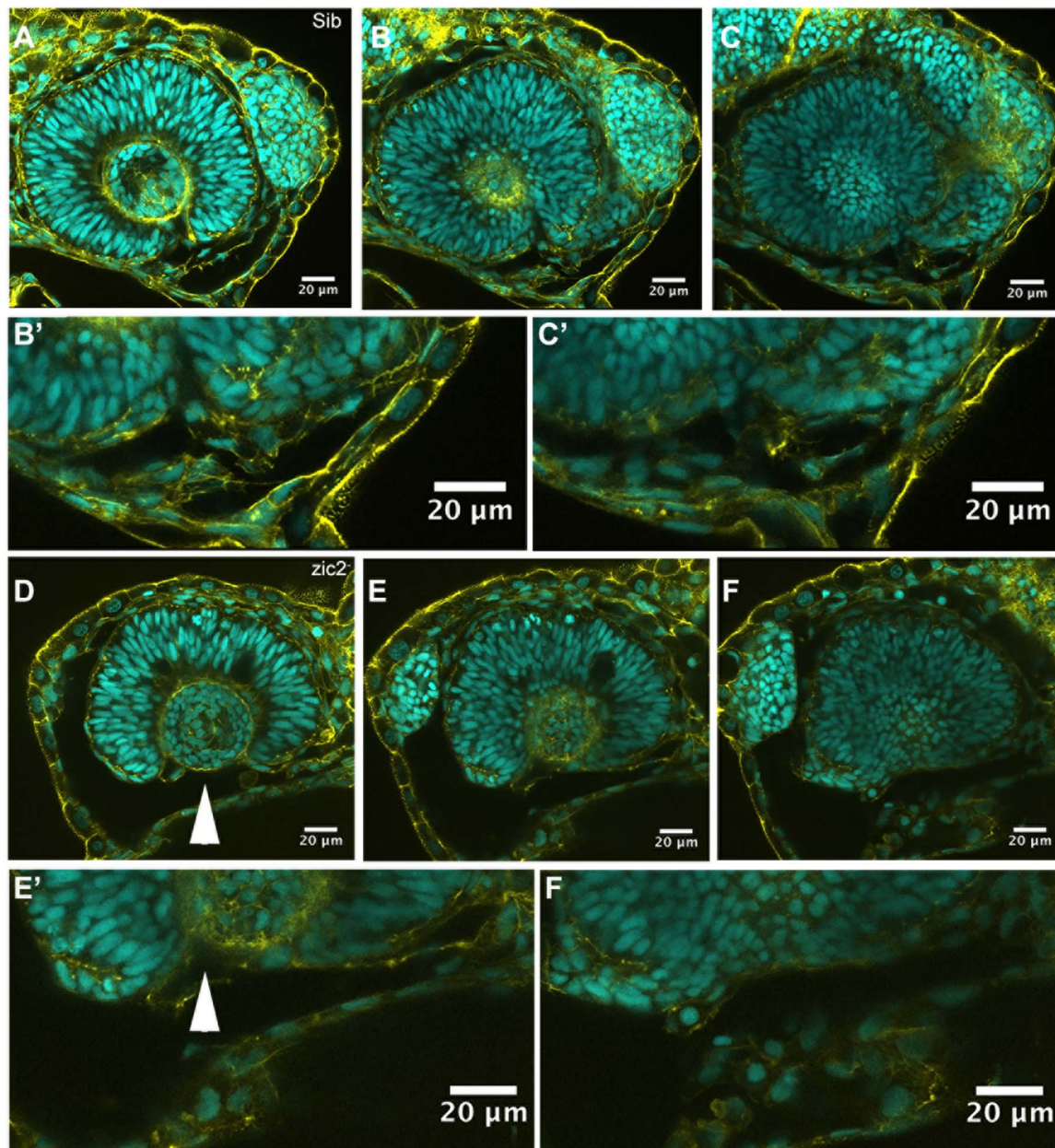


Fig. 8. Ventral periocular neural crest is depleted in MZ-*zic2* mutants. Single confocal sections through optic cups of embryos derived from *zic2a*^{gbl133}/+; *zic2b*¹¹¹⁶/*zic2b*¹¹¹⁶ parents. A–C': embryo with normal retinal morphology. D–F': embryo with coloboma. Embryos were imaged in lateral mounts. Cyan = nuclei visualized by DAPI; yellow=F-actin cytoskeleton visualized by phalloidin. Arrowheads point to aberrant gap in the ventral retina (coloboma). Embryos are shown in lateral views, anterior to the right (A–C) or anterior to the left (E–G). B', C', E', F' are enlarged from B, C, E and F, respectively.

(Evans and Gage, 2005; Matt et al., 2008) and in zebrafish morpholino knockdowns (Lupo et al., 2011; McMahon et al., 2009). There is yet much to learn about the mechanisms of these cell interaction, e.g. which specific neural crest lineages are important, when and how they interact with the retina, and which genes direct these interactions. Addressing these questions in robust mutant-based models will be essential going forward, yet such models are currently few and far between. The *zic2* mutant zebrafish is an important step toward filling this gap.

Genetic removal of maternal *zic2b* enhances penetrance and expressivity of retinal coloboma in *zic2* mutant embryos (Fig. 1), suggesting a potential requirement for zebrafish *zic2* function during gastrulation. *Zic2a* and *2b* are expressed in the gastrula mesoderm (Drummond et al., 2013; Grinblat and Sive, 2001; Toyama et al., 2004), including the prechordal plate, which induces formation of the hypothalamus in the ventral diencephalon (Mathieu et al., 2002; Pera

and Kessel, 1997; Rubenstein et al., 1998). The hypothalamus subsequently becomes an important source of Shh and is required for regionalization of the anterior diencephalon and optic fissure (Shimamura and Rubenstein, 1997; Zhao et al., 2012). It is therefore feasible that *zic2* functions in the prechordal plate during gastrulation to promote ventral diencephalic/hypothalamic specification and the establishment of the hypothalamic signaling center. This hypothesis is supported by the partial rescue of coloboma by Hh inhibition in MZ-*zic2* mutants. Notably, mouse *zic2* promotes formation of the embryonic organizer during gastrulation (Barratt et al., 2014; Houtmeyers et al., 2016; Warr et al., 2008).

zic2a, but not *zic2b*, is also expressed in a restricted domain in the distal OS (Nyholm et al., 2007; Sanek et al., 2009; Toyama et al., 2004), where it may function to promote choroid fissure formation cell-autonomously. However, *zic2b* function should then be largely dispensable for normal retinal morphogenesis; this prediction is not born

out by our results, which instead point toward a strict requirement for *zic2b* and a somewhat relaxed requirement for *zic2a* function during retinal morphogenesis (Fig. 1).

zic2a and *zic2b* are also expressed in the retina itself, as is *zic2* in higher vertebrates (Brown et al., 2003; Nagai et al., 1997; Toyama et al., 2004). While this expression begins relatively late, ~ 24 hpf, it may contribute to retinal morphogenesis cell-autonomously. The timing of the *zic2* mutant deficits described here, which manifest by 24 hpf, argues against a cell-autonomous function of *zic2* in the retina. However, the accumulated evidence in mouse models warrants a detailed examination of retinal function of zebrafish *zic2* (Garcia-Frigola et al., 2008; Herrera et al., 2003; Lee et al., 2008b). *zic2* mutants in combination with powerful methodologies available in zebrafish, e.g. transplant assays, tissue-specific transgenesis and high-resolution live imaging, provide a robust platform for testing these hypotheses efficiently in future studies.

3.2. What is the molecular mechanism of *zic2* function in the developing retina?

Misregulation of PAX2 has been causally linked to coloboma in humans (reviewed in Gregory-Evans et al. (2004)) and in chick (Sehgal et al., 2008). Regardless of the cell type where *zic2* exerts its primary function, it is likely that misregulation of *pax2a* in *zic2* mutants demonstrated here and in *zic2* morphants (Sanek et al., 2009) contributes to their retinal anomalies; for this reason, it will be important to ask if this mechanism is conserved in mouse models.

Our demonstration that cyclopamine exposure ameliorates *zic2*-linked coloboma supports, albeit indirectly, the idea that Hh signaling upregulation is responsible for retinal defects in *zic2* mutants. *pax2a*, a target of Hh signaling, is mispatterned, but is not reduced overall in *zic2* mutants. Likewise, upregulation of Hh signaling is not detectable at the level of whole-transcriptome gene expression of known direct targets of Hh at the diencephalic midline, *ptc1* and *nkx2.2* (Bergeron et al., 2008). These genes are also expressed normally in *zic2* mutants when assayed by WISH (data not shown).

An alternate hypothesis, consistent with the apparent de-repression of Hh signaling in *zic2* mutants posits that *Zic2* regulates transcription of Hh pathway components in a small portion of the embryo, such that would not be detected by our whole-embryo transcriptome approach. For example, it is plausible that a sub-lineage of the periocular neural crest modulates Hh signaling by producing secreted Hh inhibitors or creating physical barriers for Hh diffusion. It is also possible that *zic2* restricts *pax2a* transcription via a parallel, Hh-independent mechanism. If this were the case, cyclopamine acting through Hh signaling may counteract *pax2a* expansion in *zic2* mutants, thereby alleviating severity of coloboma observed in MZ-*zic2* mutants. Our data are also consistent with the possibility that *zic2* controls cell movements of *pax2a*-expressing cells rather than *pax2a* transcription. While the apparent increase in the number of *pax2a*-positive cells in the mutant diencephalon (Fig. 3G-I) argues against this hypothesis, additional studies are needed to test these hypotheses.

We have likely missed important targets of *zic2* in our whole-embryo transcriptome analysis. In other contexts, *zic2* has been shown to directly modulate Nodal signaling and canonical Wnt signaling (Fujimi et al., 2012; Houtmeyers et al., 2016; Murgan et al., 2015; Pourebrahim et al., 2011) and may function in this capacity in the developing zebrafish. Exciting recent data identify *Zic2* as a key co-factor for chromatin remodeling in embryonic stem cells (Luo et al., 2015), and may function in this capacity in the developing embryos. Nonetheless, the broad-stroke approach taken here has correctly identified a number of cell lineages that depend on *zic2* function, among them periocular neural crest, which is necessary for the formation and subsequent closure of the choroid fissure and whose migration is guided by the optic vesicle and by the optic stalks (Eberhart et al., 2008; Langenberg et al., 2008). Despite its limitations,

this approach has led us to identify a strong candidate effector of *zic2* function in retinal and craniofacial development, *alx1*. Going forward, RNA-seq to MZ-*zic2* embryos at earlier stages of development will allow identification of a more complete and focused set of proximal *zic2* targets and effectors.

3.3. How does this work inform our understanding of mammalian HPE and related disorders?

Loss-of-function alleles of *ZIC2* are found in 10% of patients with the HPE (Brown et al., 2005; Solomon et al., 2010). *zic2*-linked HPE is unusual for two reasons. First, its penetrance in human patients is the highest of the common HPE-linked genes, 87%; by comparison, penetrance of HPE in patients with *Shh* mutations is only 36% (Solomon et al., 2012). Second, in contrast to *Shh*-linked HPE, facial structures of *zic2*-linked HPE patients are largely normal, although their cerebral morphology ranges from microform to severe alobar (Solomon et al., 2010). This suggests that the developing human forebrain is very sensitive to reduction in *ZIC2* levels during human embryogenesis (in contrast, duplication of the *ZIC2*-containing region does not disrupt human development (Jobanputra et al., 2012)).

Mouse and zebrafish embryos are less sensitive to *zic2* depletion, since they develop normally when heterozygous for loss-of-function alleles of *zic2*. Coloboma is the most obvious defect in zebrafish that lack *zic2*, but diencephalic deficits are also present, as indicated by dysmorphic preoptic diencephalon (Fig. 3), narrowing of forebrain midline in the MZ-*zic2* mutants (Fig. 1) and reduction of ventral diencephalic marker expression in *zic2* mutants (e.g. *lhx6* and *nkx2.1*; Fig. S3). In contrast, homozygous *zic2* mouse mutants develop with prominent forebrain defects (Elms et al., 2003; Nagai et al., 2000). Gongal et al. (2011) have proposed that HPE and coloboma represent mild and severe aspects of the same phenotypic spectrum; by this token, it is likely that the overt differences between mouse and zebrafish mutant phenotypes reflect quantitative rather than qualitative differences in brain primordium architecture in teleosts vs mammals. This argument further emphasizes the need for in-depth analysis of *zic2* functions in more than one model organism.

It is important to note that *zic2* double mutant phenotypes largely, but not completely, replicate the phenotypes observed after morpholino-mediated knockdown of *zic2a* and *zic2b* individually. The biggest difference between the assays is observed in the anterior diencephalon, which forms normally in MZ-*zic2* mutants (Fig. 3), but is disrupted in *zic2a* morphants (Sanek and Grinblat, 2008; Sanek et al., 2009; Teslaa et al., 2013). This difference may indicate genetic compensation by other members of the zebrafish *Zic* family that function during brain morphogenesis (Elsen et al., 2008; Maurus and Harris, 2009; Winata et al., 2013) and retinal morphogenesis (Maurus and Harris, 2009). More generally, this study demonstrates the ability of closely related orthologs to compensate for each other's functions when disrupted chromosomally, but not via transient knockdown. These data will contribute to the collective efforts to understand the mechanisms that underlie the well-documented differences in outcomes of gene disruption through transient knockdown and chromosomal lesions in target genes (Kok et al., 2015; Rossi et al., 2015).

Collectively, our data identify a novel role for *zic2* in frontonasal/periocular neural crest development and establish a new animal model of inherited coloboma with frontonasal dysplasia. These data suggest that *ZIC2* mutations may contribute to human conditions other than HPE, e.g. frontonasal dysplasia. Human hereditary coloboma frequently presents unilaterally, an indication that modifiers (genetic or environmental) are important contributors to choroid fissure formation. We find that coloboma in zygotic *zic2* mutants is incompletely penetrant and predominantly unilateral, making this model ideally suited for modifier screens to identify molecular pathways that interact with *zic2*. This model will also facilitate in-depth analysis of other key roles for *zic2*, e.g. their functions in post-mitotic neurons such as

cerebellar granule neurons (Frank et al., 2015) and Cajal–Retzius cells (Escalante et al., 2013; Murillo et al., 2015) and its potential link to schizophrenia (Hatayama et al., 2011).

4. Materials and methods

4.1. Zebrafish strains and embryo manipulation

Adult zebrafish were maintained according to established methods (Westerfield, 1993). All experimental protocols using zebrafish were approved by the University of Wisconsin Animal Care and Use Committee, and carried out in accordance with the institutional animal care protocols. Embryos were obtained from natural matings and staged according to Kimmel et al. (1995). The following mutant strains of zebrafish were used: *zic2a*^{GBT133} insertional mutant (Clark et al., 2011); *zic2b*^{UW1104} mutant, generated by TALEN mutagenesis in the course of the study; *zic2b*^{UW1127} and *zic2b*^{UW1116} mutants, generated by CRISPR/Cas9 mutagenesis in the course of this study. Double *zic2* mutants were obtained by crossing *zic2a*^{GBT133} /+ zebrafish to each of the three *zic2* mutant allele carriers; F1s were selected by RFP fluorescence to identify *zic2a*^{GBT133} carriers, which express RFP (Clark et al., 2011) and raised to adulthood. Adult *zic2b*+/− zebrafish were identified by PCR genotyping of genomic DNA extracted from tail clips.

Cyclopamine treatments were carried out as follows: Cyclopamine (AdipoGen) was diluted in DMSO and added to E3 to final concentrations of 3uM or 4.5uM; final DMSO concentration was adjusted to 0.5%. Embryos were placed in E3 with cyclopamine or 0.5%DMSO for vehicle-only control. Treatments were started at 3hpf (before maternal-zygotic transition), 5 hpf or 6hpf. Embryos were moved to fresh E3 at 24 hpf and allowed to develop until 3–4 dpf, when they were assayed for retinal morphology.

4.2. Engineered nuclease mutagenesis and high-resolution melt analysis (HRMA)

Zic2b TALEN was designed and synthesized by the Mutation Generation and Detection Core (MGD) Facility, University of Utah to the following target left and right sites in exon 1, respectively: 5'-TCCTCTGCGCAGCCGAGG-3' and 5'-GGGTGTTGTCCACTGGCCG-3'.

Design of *zic2b* CRISPR site 5'-GGTGGAGTTAAAAGTGGAGC-3' in exon1, mutagenesis and founder identifications were carried out as previously described (Sedyk et al., 2016), with the following HRMA primers pairs: TALEN site - 5'-TGGACAACACCCCATCTTCA-3' and 5'-GGATGTTTGGAGAGCCGTGAT-3'; CRISPR site - 5'-TATTCTGCGGCCGCTCTT3' and 5'-GGAGTCGAATCCCCAAATC-3'.

4.3. Sequencing and PCR genotyping of *zic2* mutant alleles

To determine *zic2a* genotype, DNA was extracted from individual embryos or adult fish and subjected to PCR with the following primers: *gbt* forward 5'-CCCCGTAATGCAGAAGAAGA-3', *gbt* reverse 5'-GTCCAGCTTGATGTCGGTCT-3', *wt* forward and *wt* reverse 5'-ATTTCATGGAGCCGTACTGTTGTG-3' and 5'-TGTTACTGGACGCAGGCATCAGTT-3'. (see Supp. Fig. 2 for details).

Zic2b PCR fragments identified as mutant by HRMA were subcloned via TA cloning into pGEMT-Easy (Promega) and sequenced to characterize the mutations. Subsequently, PCR followed by Metaphor gel electrophoresis was used to efficiently genotype individual embryos and adult fish, HRMA primer sequence above were used for CRISPR allele genotyping. TALEN allele genotyping used 5'-GGACAACACCCCATCTTC-3' and 5'-CGGGGAAAAGTAGGTGAC-3' (Supp. Fig. 2).

4.4. RNA-seq transcriptome analysis

Embryos derived from a *zic2a*^{GBT133}/+; *zic2b*^{UW1127}/+ incross were sorted by presence or absence of coloboma. RNA was prepared from

each individual embryo using the RNaseasy kit (Qiagen) according to (de Jong et al., 2010). cDNA libraries were prepared using the TruSeq stranded mRNA library preparation protocol with poly-A selection and sequenced on the Illumina HiSeq. 2500. Gene-level read counts were estimated from the raw sequencing data using RSEM v1.2.18 (Li and Dewey, 2011) and Bowtie v1.1.1 (Langmead et al., 2009). The gene set used consisted of all genes classified as protein coding or lincRNA within the Ensembl v77 annotation of the Zv9 assembly of the zebrafish genome. RSEM was run with option “-forward-prob 0” to take into account that the RNA-seq libraries were strand-specific. A matrix of gene-level counts from all libraries was compiled and analyzed for differential gene expression using the R statistical language and environment (R core team, 2014). Specifically, the count matrix was first pre-normalized using the median normalization routine from the EBSeq v1.5.4 package (Leng et al., 2013). The normalized dataset was then filtered to exclude genes that did not show coverage of at least 10 counts in at least 1 library across the entire dataset. The edgeR v3.14.0 package, (Robinson et al., 2010) with internal normalization switched off, was subsequently applied to call for differential expression (DE). Genes with assigned value of False Discovery Rate (FDR) below 0.05 by edgeR were preliminarily selected. Since a) low-expressed genes tend to be artificially enriched in the list of genes called DE by statistical algorithms and b) DE genes expressed at higher levels have more biological relevance and follow-up potential, we applied an additional filter to the edgeR output by retaining genes that have expression exceeding a certain quantile (0.2) of genome-wide distribution of expression values in at least 60% of libraries representing the strain with a larger mean expression of that gene.

4.5. Immunohistochemistry, in situ hybridization and Alcian Blue staining

Embryos were fixed in 4% paraformaldehyde (PFA) in PBS, or in 4% PFA/0.25% glutaraldehyde, 5 mM EGTA, 0.2% TritonX-100, 1xPBS for optimal phalloidin staining. After PFA/glutaraldehyde fix, embryos were treated with 100 mM sodium borohydride to reduce auto-fluorescence. Primary antibodies were detected fluorescently with Alexa-labeled goat anti-mouse or goat anti-rabbit secondary antibodies. Embryos were mounted in VectaShield and imaged on an Olympus IX81 inverted confocal microscope with the Fluoview 1000 confocal package, using a 60× water immersion objective (NA 1.10), a 60× oil immersion objective (NA 1.35) or a 20× objective (NA 0.75).

Antibody/ stain reagent	Source	Dilution
Rabbit anti-pax2a	GeneTex, cat# GTX128127	1:500
Mouse anti-acetylated tubulin	Sigma, T6793	1:400
Goat Anti-Mouse Alexa 488	Invitrogen, cat#A-11001	1:500
Goat Anti-Rabbit Alexa 568	Invitrogen, cat#A-11011	1:500
phalloidin Alexa 488 or 568	Molecular Probes, cat#A12379; A12380	1:100
DAPI	Molecular Probes, cat#D21490	1:5000

In situ hybridization was carried out as previously described (Gillhouse et al., 2004), using the following probes: *pax2a* (Hoyle et al., 2004); *dlx2a* (Akimenko et al., 1994); *crestin* (Luo et al., 2001); *vax2* (Gross and Dowling, 2005); *atoh7* (Masai et al., 2000). *cln11a* was synthesized as a gBlocks® Gene Fragments (IDT) and TA-cloned into pGEMT-Easy (Promega). Full length *alx1* cDNA was amplified from total mRNA of 24 hpf embryos by PCR with primers 5'-TTGAGACGAGGCCAGAGGAC-3' and 5'-CCTGGCTCTGTGAATAA-

TTACAAG-3' primers using OneTaq One-Step RT-PCR kit (NEB), and TA-cloned into pGEMT-Easy (Promega). After WISH, embryos were mounted in 100% glycerol and imaged on Axioskop2 Plus (Zeiss) compound or Leica MZ FLIII stereo microscopes equipped with Leica DFC310 FX camera and LAS v4.0 software. For cartilage staining, zebrafish larvae were fixed at 5–6 dpf in 4% paraformaldehyde and stained with Alcian Blue according to (Kimmel et al., 1998). Samples were flat-mounted in glycerol for imaging as described above.

Competing interests

No competing interests declared.

Author contributions

The study was designed by YG. IS, BY and LR carried out the bulk of the experiments. IS, BY and YG analyzed the data. OM and CD carried out bioinformatic analysis of RNAseq data. YG, IS and BY wrote the manuscript. All authors approved the manuscript prior to submission.

Funding

This work was supported by grants from the National Institutes of Health (EY022098-01) and American Heart Association (11GRNT-7770002) to Y.G, and the Vilas Trust.

Data availability

Original data in support of this publication is available upon request. The RNA-seq data files from this study have been deposited at the National Center for Biotechnology Information Gene Expression Omnibus (NCBI GEO) database (accession number GSE99382).

Acknowledgements

We are grateful to Abby Keller for establishing technical expertise in CRISPR mutagenesis, Kelsey Baubie and Lizzie Roehl for fish husbandry. We thank Steve Ekker for providing the *zic2a*^{gbl133} mutant zebrafish and Kristen Kwan for the gift of *pax2a* antibody. We also wish to thank David Grunwald for advice and support, the University of Utah Mutation Generation and Detection Core for TALEN design, and the University of Wisconsin Biotechnology Center DNA Sequencing Facility for providing sequencing facilities and services.

Appendix A. Supplementary material

Supplementary data associated with this article can be found in the online version at <http://dx.doi.org/10.1016/j.ydbio.2017.07.003>.

References

- Akimenko, M.A., Ekker, M., Wegner, J., Lin, W., Westerfield, M., 1994. Combinatorial expression of three zebrafish genes related to distal-less: part of a homeobox gene code for the head. *J. Neurosci.* 14, 3475–3486.
- Barratt, K.S., Glanville-Jones, H.C., Arkell, R.M., 2014. The *Zic2* gene directs the formation and function of node cilia to control cardiac situs. *Genesis* 52, 626–635.
- Bazin-Lopez, N., Valdivia, L.E., Wilson, S.W., Gestri, G., 2015. Watching eyes take shape. *Curr. Opin. Genet. Dev.* 32, 73–79.
- Bergeron, S.A., Milla, L.A., Villegas, R., Shen, M.C., Burgess, S.M., Allende, M.L., Karlstrom, R.O., Palma, V., 2008. Expression profiling identifies novel Hh/Gli-regulated genes in developing zebrafish embryos. *Genomics* 91, 165–177.
- Bertola, D.R., Rodrigues, M.G., Quaio, C.R., Kim, C.A., Passos-Bueno, M.R., 2013. Vertical transmission of a frontonasal phenotype caused by a novel *ALX4* mutation. *Am. J. Med. Genet. Part A* 161A, 600–604.
- Bronstein, J.M., Micevich, P.E., Chen, K., 1997. Oligodendrocyte-specific protein (OSP) is a major component of CNS myelin. *J. Neurosci. Res.* 50, 713–720.
- Brown, L., Paraso, M., Arkell, R., Brown, S., 2005. In vitro analysis of partial loss-of-function *ZIC2* mutations in holoprosencephaly: alanine tract expansion modulates DNA binding and transactivation. *Human. Mol. Genet.* 14, 411–420.
- Brown, L.Y., Kottmann, A.H., Brown, S., 2003. Immunolocalization of *Zic2* expression in the developing mouse forebrain. *Gene Expr. Patterns* 3, 361–367.
- Brown, L.Y., Odent, S., David, V., Blayau, M., Dubourg, C., Apacik, C., Delgado, M.A., Hall, B.D., Reynolds, J.F., Sommer, A., Wiczorek, D., Brown, S.A., Muenke, M., 2001. Holoprosencephaly due to mutations in *ZIC2*: alanine tract expansion mutations may be caused by parental somatic recombination. *Human. Mol. Genet.* 10, 791–796.
- Brown, S.A., Warburton, D., Brown, L.Y., Yu, C.Y., Roeder, E.R., Stengel-Rutkowski, S., Hennekam, R.C., Muenke, M., 1998. Holoprosencephaly due to mutations in *ZIC2*, a homologue of *Drosophila odd-paired*. *Nat. Genet.* 20, 180–183.
- Brugmann, S.A., Allen, N.C., James, A.W., Mekonnen, Z., Madan, E., Helms, J.A., 2010. A primary cilia-dependent etiology for midline facial disorders. *Hum. Mol. Genet.* 19, 1577–1592.
- Cannon, J.E., Place, E.S., Eve, A.M., Bradshaw, C.R., Sesay, A., Morrell, N.W., Smith, J.C., 2013. Global analysis of the haematopoietic and endothelial transcriptome during zebrafish development. *Mech. Dev.* 130, 122–131.
- Clark, K.J., Balcunas, D., Pogoda, H.M., Ding, Y., Westcot, S.E., Bedell, V.M., Greenwood, T.M., Urban, M.D., Skuster, K.J., Petzold, A.M., Ni, J., Nielsen, A.L., Patowary, A., Scaria, V., Sivasubbu, S., Xu, X., Hammerschmidt, M., Ekker, S.C., 2011. In vivo protein trapping produces a functional expression codex of the vertebrate proteome. *Nat. Methods* 8, 506–515.
- Couly, G., Creuzet, S., Bennaceur, S., Vincent, C., Le Douarin, N.M., 2002. Interactions between Hox-negative cephalic neural crest cells and the foregut endoderm in patterning the facial skeleton in the vertebrate head. *Development* 129, 1061–1073.
- de Jong, M., Rauwerda, H., Bruning, O., Verkooijen, J., Spaik, H.P., Breit, T.M., 2010. RNA isolation method for single embryo transcriptome analysis in zebrafish. *BMC Res. Notes* 3, 73.
- Dee, C.T., Szymoniuk, C.R., Mills, P.E., Takahashi, T., 2013. Defective neural crest migration revealed by a Zebrafish model of *Alx1*-related frontonasal dysplasia. *Hum. Mol. Genet.* 22, 239–251.
- Drummond, D.L., Cheng, C.S., Selland, L.G., Hocking, J.C., Prichard, L.B., Waskiewicz, A.J., 2013. The role of *Zic* transcription factors in regulating hindbrain retinoic acid signaling. *BMC Dev. Biol.* 13, 31.
- Eberhart, J.K., He, X., Swartz, M.E., Yan, Y.L., Song, H., Boling, T.C., Kunerth, A.K., Walker, M.B., Kimmel, C.B., Postlethwait, J.H., 2008. *MicroRNA Mirm140* modulates *Pdgfr* signaling during palatogenesis. *Nat. Genet.* 40, 290–298.
- Ekker, S.C., Ungar, A.R., Greenstein, P., von Kessler, D.P., Porter, J.A., Moon, R.T., Beachy, P.A., 1995. Patterning activities of vertebrate hedgehog proteins in the developing eye and brain. *Curr. Biol.* 5, 944–955.
- Elms, P., Scurry, A., Davies, J., Willoughby, C., Hacker, T., Bogani, D., Arkell, R., 2004. Overlapping and distinct expression domains of *Zic2* and *Zic3* during mouse gastrulation. *Gene Expr. Patterns* 4, 505–511.
- Elms, P., Siggers, P., Napper, D., Greenfield, A., Arkell, R., 2003. *Zic2* is required for neural crest formation and hindbrain patterning during mouse development. *Dev. Biol.* 264, 391–406.
- Elsen, G.E., Choi, L.Y., Millen, K.J., Grinblat, Y., Prince, V.E., 2008. *Zic1* and *Zic4* regulate zebrafish roof plate specification and hindbrain ventricle morphogenesis. *Dev. Biol.* 314, 376–392.
- Escalante, A., Murillo, B., Morenilla-Palao, C., Klar, A., Herrera, E., 2013. *Zic2*-dependent axon midline avoidance controls the formation of major ipsilateral tracts in the CNS. *Neuron* 80, 1392–1406.
- Evans, A.L., Gage, P.J., 2005. Expression of the homeobox gene *Pitx2* in neural crest is required for optic stalk and ocular anterior segment development. *Hum. Mol. Genet.* 14, 3347–3359.
- Frank, C.L., Liu, F., Wijayathunge, R., Song, L., Biegler, M.T., Yang, M.G., Vockley, C.M., Safi, A., Gersbach, C.A., Crawford, G.E., West, A.E., 2015. Regulation of chromatin accessibility and *Zic* binding at enhancers in the developing cerebellum. *Nat. Neurosci.* 18, 647–656.
- Fujimi, T.J., Hatayama, M., Aruga, J., 2012. *Xenopus Zic3* controls notochord and organizer development through suppression of the Wnt/beta-catenin signaling pathway. *Dev. Biol.* 361, 220–231.
- Garcia-Frigola, C., Carreres, M.I., Vegar, C., Mason, C., Herrera, E., 2008. *Zic2* promotes axonal divergence at the optic chiasm midline by EphB1-dependent and -independent mechanisms. *Development* 135, 1833–1841.
- Gestri, G., Link, B.A., Neuhaus, S.C., 2012. The visual system of zebrafish and its use to model human ocular diseases. *Dev. Neurobiol.* 72, 302–327.
- Gillhouse, M., Wagner Nyholm, M., Hikasa, H., Sokol, S.Y., Grinblat, Y., 2004. Two *Frodo/Dapper* homologs are expressed in the developing brain and mesoderm of zebrafish. *Dev. Dyn.* 230, 403–409.
- Gongal, P.A., French, C.R., Waskiewicz, A.J., 2011. Aberrant forebrain signaling during early development underlies the generation of holoprosencephaly and coloboma. *Biochim. Biophys. Acta* 1812, 390–401.
- Gregory-Evans, C.Y., Williams, M.J., Halford, S., Gregory-Evans, K., 2004. Ocular coloboma: a reassessment in the age of molecular neuroscience. *J. Med. Genet.* 41, 881–891.
- Grinblat, Y., Sive, H., 2001. *zic* Gene expression marks anteroposterior pattern in the presumptive neuroectoderm of the zebrafish gastrula. *Dev. Dyn.* 222, 688–693.
- Gross, J.M., Dowling, J.E., 2005. *Tbx2b* is essential for neuronal differentiation along the dorsal/ventral axis of the zebrafish retina. *Proc. Natl. Acad. Sci. USA* 102, 4371–4376.
- Hatayama, M., Ishiguro, A., Iwayama, Y., Takashima, N., Sakoori, K., Toyota, T., Nozaki, Y., Odaka, Y.S., Yamada, K., Yoshikawa, T., Aruga, J., 2011. *Zic2* hypomorphic mutant yic as a schizophrenia model and *ZIC2* mutations identified in schizophrenia patients. *Sci. Rep.* 1, 16.
- Herrera, E., Brown, L., Aruga, J., Rachel, R.A., Dolen, G., Mikoshiba, K., Brown, S., Mason, C.A., 2003. *Zic2* patterns binocular vision by specifying the uncrossed retinal projection. *Cell* 114, 545–557.

- Houtmeyers, R., Tchouate Gainkam, O., Glanville-Jones, H.A., Van den Bosch, B., Chappell, A., Barratt, K.S., Souopgui, J., Tejpar, S., Arkell, R.M., 2016. Zic2 mutation causes holoprosencephaly via disruption of NODAL signalling. *Hum. Mol. Genet.* 25, 3946–3959.
- Hoyle, J., Tang, Y.P., Wietzel, E.L., Wardle, F.C., Sive, H., 2004. *nlz* gene family is required for hindbrain patterning in the zebrafish. *Dev. Dyn.* 229, 835–846.
- Huang da, W., Sherman, B.T., Lempicki, R.A., 2009. Systematic and integrative analysis of large gene lists using DAVID bioinformatics resources. *Nat. Protoc.* 4, 44–57.
- Inoue, T., Ota, M., Mikoshiba, K., Aruga, J., 2007. Zic2 and Zic3 synergistically control neurulation and segmentation of paraxial mesoderm in mouse embryo. *Dev. Biol.* 306, 669–684.
- Jobanputra, V., Burke, A., Kwame, A.Y., Shanmugham, A., Shirazi, M., Brown, S., Warburton, P.E., Levy, B., Warburton, D., 2012. Duplication of the ZIC2 gene is not associated with holoprosencephaly. *Am. J. Med. Genet. Part A* 158A, 103–108.
- Kimmel, C.B., Ballard, W.W., Kimmel, S.R., Ullmann, B., Schilling, T.F., 1995. Stages of embryonic development of the zebrafish. *Dev. Dyn.* 203, 253–310.
- Kimmel, C.B., Miller, C.T., Krueze, G., Ullmann, B., BreMiller, R.A., Larison, K.D., Snyder, H.C., 1998. The shaping of pharyngeal cartilages during early development of the zebrafish. *Dev. Biol.* 203, 245–263.
- Kish, P.E., Bohnsack, B.L., Gallina, D., Kasprick, D.S., Kahana, A., 2011. The eye as an organizer of craniofacial development. *Genesis* 49, 222–230.
- Kok, F.O., Shin, M., Ni, C.W., Gupta, A., Grosse, A.S., van Impel, A., Kirchmaier, B.C., Peterson-Maduro, J., Kourkoulis, G., Male, I., DeSantis, D.F., Sheppard-Tindell, S., Ebarasi, L., Betsholtz, C., Schulte-Merker, S., Wolfe, S.A., Lawson, N.D., 2015. Reverse genetic screening reveals poor correlation between morpholino-induced and mutant phenotypes in zebrafish. *Dev. Cell* 32, 97–108.
- Kwan, K.M., 2014. Coming into focus: the role of extracellular matrix in vertebrate optic cup morphogenesis. *Dev. Dyn.* 243, 1242–1248.
- Lakhwani, S., Garcia-Sanz, P., Vallejo, M., 2010. *Alx3*-deficient mice exhibit folic acid-resistant craniofacial midline and neural tube closure defects. *Dev. Biol.* 344, 869–880.
- Langenberg, T., Kahana, A., Wszalek, J.A., Halloran, M.C., 2008. The eye organizes neural crest cell migration. *Dev. Dyn.* 237, 1645–1652.
- Langmead, B., Trapnell, C., Pop, M., Salzberg, S.L., 2009. Ultrafast and memory-efficient alignment of short DNA sequences to the human genome. *Genome Biol.* 10, R25.
- Le Douarin, N.M., Brito, J.M., Creuzet, S., 2007. Role of the neural crest in face and brain development. *Brain Res. Rev.* 55, 237–247.
- Lee, J., Willer, J.R., Willer, G.B., Smith, K., Gregg, R.G., Gross, J.M., 2008a. Zebrafish blowout provides genetic evidence for Patched1-mediated negative regulation of Hedgehog signaling within the proximal optic vesicle of the vertebrate eye. *Dev. Biol.* 319, 10–22.
- Lee, R., Petros, T.J., Mason, C.A., 2008b. Zic2 regulates retinal ganglion cell axon avoidance of ephrinB2 through inducing expression of the guidance receptor EphB1. *The J. Neurosci.* 28, 5910–5919.
- Leng, N., Dawson, J.A., Thomson, J.A., Ruotti, V., Rissman, A.I., Smits, B.M., Haag, J.D., Gould, M.N., Stewart, R.M., Kendziora, C., 2013. EBSeq: an empirical Bayes hierarchical model for inference in RNA-seq experiments. *Bioinformatics* 29, 1035–1043.
- Li, B., Dewey, C.N., 2011. RSEM: accurate transcript quantification from RNA-Seq data with or without a reference genome. *BMC Bioinform.* 12, 323.
- Luo, R., An, M., Arduini, B.L., Henion, P.D., 2001. Specific pan-neural crest expression of zebrafish *Crestin* throughout embryonic development. *Dev. Dyn.* 220, 169–174.
- Luo, Z., Gao, X., Lin, C., Smith, E.R., Marshall, S.A., Swanson, S.K., Florens, L., Washburn, M.P., Shilatifard, A., 2015. Zic2 is an enhancer-binding factor required for embryonic stem cell specification. *Mol. Cell* 57, 685–694.
- Lupo, G., Gestri, G., O'Brien, M., Denton, R.M., Chandraratna, R.A., Ley, S.V., Harris, W.A., Wilson, S.W., 2011. Retinoic acid receptor signaling regulates choroid fissure closure through independent mechanisms in the ventral optic cup and periorbital mesenchyme. *Proc. Natl. Acad. Sci. USA* 108, 8698–8703.
- Lupo, G., Liu, Y., Qiu, R., Chandraratna, R.A., Barsacchi, G., He, R.Q., Harris, W.A., 2005. Dorsorostral patterning of the *Xenopus* eye: a collaboration of Retinoid, Hedgehog and FGF receptor signaling. *Development* 132, 1737–1748.
- Macdonald, R., Barth, K.A., Xu, Q., Holder, N., Mikkola, I., Wilson, S.W., 1995. Midline signalling is required for Pax gene regulation and patterning of the eyes. *Development* 121, 3267–3278.
- Masai, I., Stemple, D.L., Okamoto, H., Wilson, S.W., 2000. Midline signals regulate retinal neurogenesis in zebrafish. *Neuron* 27, 251–263.
- Mathieu, J., Barth, A., Rosa, F.M., Wilson, S.W., Peyrieras, N., 2002. Distinct and cooperative roles for Nodal and Hedgehog signals during hypothalamic development. *Development* 129, 3055–3065.
- Matt, N., Ghyselinck, N.B., Pellerin, I., Dupe, V., 2008. Impairing retinoic acid signalling in the neural crest cells is sufficient to alter entire eye morphogenesis. *Dev. Biol.* 320, 140–148.
- Maurus, D., Harris, W.A., 2009. Zic-associated holoprosencephaly: zebrafish Zic1 controls midline formation and forebrain patterning by regulating Nodal, Hedgehog, and retinoic acid signaling. *Genes Dev.* 23, 1461–1473.
- McMahon, C., Gestri, G., Wilson, S.W., Link, B.A., 2009. *Lmx1b* is essential for survival of periorbital mesenchymal cells and influences Fgf-mediated retinal patterning in zebrafish. *Dev. Biol.* 332, 287–298.
- Morita, K., Sasaki, H., Fujimoto, K., Furuse, M., Tsukita, S., 1999. Claudin-11/OSP-based tight junctions of myelin sheaths in brain and Sertoli cells in testis. *J. Cell Biol.* 145, 579–588.
- Mui, S.H., Kim, J.W., Lemke, G., Bertuzzi, S., 2005. Vax genes ventralize the embryonic eye. *Genes Dev.* 19, 1249–1259.
- Murgan, S., Kari, W., Rothbacher, U., Iche-Torres, M., Melenc, P., Hobert, O., Bertrand, V., 2015. Atypical transcriptional activation by TCF via a zic transcription factor in *C. elegans* neuronal precursors. *Dev. Cell* 33, 737–745.
- Murillo, B., Ruiz-Reig, N., Herrera, M., Fairen, A., Herrera, E., 2015. Zic2 controls the migration of specific neuronal populations in the developing forebrain. *J. Neurosci.* 35, 11266–11280.
- Nagai, T., Aruga, J., Minowa, O., Sugimoto, T., Ohno, Y., Noda, T., Mikoshiba, K., 2000. Zic2 regulates the kinetics of neurulation. *Proc. Natl. Acad. Sci. USA* 97, 1618–1623.
- Nagai, T., Aruga, J., Takada, S., Gunther, T., Sporle, R., Schughart, K., Mikoshiba, K., 1997. The expression of the mouse Zic1, Zic2, and Zic3 gene suggests an essential role for Zic genes in body pattern formation. *Dev. Biol.* 182, 299–313.
- Nakata, K., Nagai, T., Aruga, J., Mikoshiba, K., 1997. *Xenopus* Zic3, a primary regulator both in neural and neural crest development. *Proc. Natl. Acad. Sci. USA* 94, 11980–11985.
- Nakata, K., Nagai, T., Aruga, J., Mikoshiba, K., 1998. *Xenopus* Zic family and its role in neural and neural crest development. *Mech. Dev.* 75, 43–51.
- Nyholm, M.K., Abdellilah-Seyfried, S., Grinblat, Y., 2009. A novel genetic mechanism regulates dorsolateral hinge-point formation during zebrafish cranial neurulation. *J. Cell Sci.* 122, 2137–2148.
- Nyholm, M.K., Wu, S.F., Dorsky, R.I., Grinblat, Y., 2007. The zebrafish *zic2a-zic5* gene pair acts downstream of canonical Wnt signaling to control cell proliferation in the developing tectum. *Development* 134, 735–746.
- Onwochei, B.C., Simon, J.W., Bateman, J.B., Couture, K.C., Mir, E., 2000. Ocular colobomata. *Surv. Ophthalmol.* 45, 175–194.
- Pan, H., Gustafsson, M.K., Aruga, J., Tiedken, J.J., Chen, J.C., Emerson, C.P., Jr., 2011. A role for Zic1 and Zic2 in Myf5 regulation and somite myogenesis. *Dev. Biol.* 351, 120–127.
- Pera, E.M., Kessel, M., 1997. Patterning of the chick forebrain anlage by the prechordal plan. *Development* 124, 4153–4162.
- Pillai-Kastoori, L., Wen, W., Wilson, S.G., Strachan, E., Lo-Castro, A., Fichera, M., Musumeci, S.A., Lehmann, O.J., Morris, A.C., 2014. Sox11 is required to maintain proper levels of Hedgehog signaling during vertebrate ocular morphogenesis. *PLoS Genet.* 10, e1004491.
- Pourebrahim, R., Houtmeyers, R., Ghogomu, S., Janssens, S., Thelie, A., Tran, H.T., Langenberg, T., Vleminckx, K., Bellefroid, E., Cassiman, J.J., Tejpar, S., 2011. Transcription factor Zic2 inhibits Wnt/beta-catenin protein signaling. *J. Biol. Chem.* 286, 37732–37740.
- Qu, S., Tucker, S.C., Zhao, Q., deCrombrughe, B., Wisdom, R., 1999. Physical and genetic interactions between *Alx4* and *Cart1*. *Development* 126, 359–369.
- Ribeiro, L.A., Roessler, E., Hu, P., Pineda-Alvarez, D.E., Zhou, N., Jones, M., Chandrasekharappa, S., Richieri-Costa, A., Muenke, M., 2012. Comparison of mutation findings in ZIC2 between microform and classical holoprosencephaly in a Brazilian cohort. *Birth Defects Res. Part A Clin. Mol. Teratol.* 94, 912–917.
- Robinson, M.D., McCarthy, D.J., Smyth, G.K., 2010. edgeR: a Bioconductor package for differential expression analysis of digital gene expression data. *Bioinformatics* 26, 139–140.
- Roessler, E., Belloni, E., Gaudenz, K., Jay, P., Berta, P., Scherer, S.W., Tsui, L.C., Muenke, M., 1996. Mutations in the human Sonic Hedgehog gene cause holoprosencephaly. *Nat. Genet.* 14, 357–360.
- Roessler, E., Lacabanne, F., Dubourg, C., Paulussen, A., Herbergs, J., Hehr, U., Bendavid, C., Zhou, N., Ouspenskaia, M., Bale, S., Odent, S., David, V., Muenke, M., 2009. The full spectrum of holoprosencephaly-associated mutations within the ZIC2 gene in humans predicts loss-of-function as the predominant disease mechanism. *Hum. Mutat.* 30, E541–554.
- Roessler, E., Muenke, M., 2010. The molecular genetics of holoprosencephaly. *Am. J. Med. Genet. Part C. Semin. Med. Genet.* 154C, 52–61.
- Rossi, A., Kontarakis, Z., Gerri, C., Nolte, H., Holper, S., Kruger, M., Stainier, D.Y., 2015. Genetic compensation induced by deleterious mutations but not gene knockdowns. *Nature* 524, 230–233.
- Rubenstein, J.L., Shimamura, K., Martinez, S., Puellas, L., 1998. Regionalization of the prosencephalic neural plate. *Annu. Rev. Neurosci.* 21, 445–477.
- Sanek, N.A., Grinblat, Y., 2008. A novel role for zebrafish *zic2a* during forebrain development. *Dev. Biol.* 317, 325–335.
- Sanek, N.A., Taylor, A.A., Nyholm, M.K., Grinblat, Y., 2009. Zebrafish *zic2a* patterns the forebrain through modulation of Hedgehog-activated gene expression. *Development* 136, 3791–3800.
- Schilling, T.F., Concordet, J.P., Ingham, P.W., 1999. Regulation of left-right asymmetries in the zebrafish by Shh and BMP4. *Dev. Biol.* 210, 277–287.
- Schimmenti, L.A., de la Cruz, J., Lewis, S.A., Karkera, J.D., Manligas, G.S., Roessler, E., Muenke, M., 2003. Novel mutation in sonic hedgehog in non-syndromic colobomatous microphthalmia. *Am. J. Med. Genet. Part A* 116A, 215–221.
- Schmitt, E.A., Dowling, J.E., 1994. Early eye morphogenesis in the zebrafish, *Brachydanio rerio*. *J. Comp. Neurol.* 344, 532–542.
- Sedykh, I., TeSlaa, J.J., Tatarsky, R.L., Keller, A.N., Toops, K.A., Lakkaraju, A., Nyholm, M.K., Wolman, M.A., Grinblat, Y., 2016. Novel roles for the radial spoke head protein 9 in neural and neurosensory cilia. *Sci. Rep.* 6, 34437.
- Sehgal, R., Karcavich, R., Carlson, S., Belecky-Adams, T.L., 2008. Ectopic Pax2 expression in chick ventral optic cup phenocopies loss of Pax2 expression. *Dev. Biol.* 319, 23–33.
- Shimamura, K., Rubenstein, J.L., 1997. Inductive interactions direct early regionalization of the mouse forebrain. *Development* 124, 2709–2718.
- Solomon, B.D., Bear, K.A., Wyllie, A., Keaton, N.A., Dubourg, C., David, V., Mercier, S., Odent, S., Hehr, U., Paulussen, A., Clegg, N.J., Delgado, M.R., Bale, S.J., Lacabanne, F., Ardinger, H.H., Aylsworth, A.S., Bhengu, N.L., Braddock, S., Brookhyser, K., Burton, B., Gaspar, H., Grix, A., Horovitz, D., Kanetkze, E., Kayserili, H., Lev, D., Nikkel, S.M., Norton, M., Roberts, R., Saal, H., Schaefer, G.B., Schneider, A., Smith, E.K., Sowry, E., Spence, M.A., Shalev, S.A., Steiner, C.E., Thompson, E.M., Winder, T.L., Balog, J.Z., Hadley, D.W., Zhou, N., Pineda-Alvarez, D.E., Roessler, E., Muenke, M.,

- M., 2012. Genotypic and phenotypic analysis of 396 individuals with mutations in Sonic Hedgehog. *J. Med. Genet.* 49, 473–479.
- Solomon, B.D., Lachawan, F., Mercier, S., Clegg, N.J., Delgado, M.R., Rosenbaum, K., Dubourg, C., David, V., Olney, A.H., Wehner, L.E., Hehr, U., Bale, S., Paulussen, A., Smeets, H.J., Hardisty, E., Tylki-Szymanska, A., Pronicka, E., Clemens, M., McPherson, E., Hennekam, R.C., Hahn, J., Stashinko, E., Levey, E., Wieczorek, D., Roeder, E., Schell-Apacik, C.C., Booth, C.W., Thomas, R.L., Kenwick, S., Cummings, D.A., Bous, S.M., Keaton, A., Balog, J.Z., Hadley, D., Zhou, N., Long, R., Velez, J.I., Pineda-Alvarez, D.E., Odent, S., Roessler, E., Muenke, M., 2010. Mutations in ZIC2 in human holoprosencephaly: description of a novel ZIC2 specific phenotype and comprehensive analysis of 157 individuals. *J. Med. Genet.* 47, 513–524.
- Swartz, M.E., Sheehan-Rooney, K., Dixon, M.J., Eberhart, J.K., 2011. Examination of a palatogenic gene program in zebrafish. *Dev. Dyn.* 240, 2204–2220.
- Take-uchi, M., Clarke, J.D., Wilson, S.W., 2003. Hedgehog signalling maintains the optic stalk-retinal interface through the regulation of Vax gene activity. *Development* 130, 955–968.
- Teslaa, J.J., Keller, A.N., Nyholm, M.K., Grinblat, Y., 2013. Zebrafish Zic2a and Zic2b regulate neural crest and craniofacial development. *Dev. Biol.* 380, 73–86.
- Toyama, R., Gomez, D.M., Mana, M.D., Dawid, I.B., 2004. Sequence relationships and expression patterns of zebrafish zic2 and zic5 genes. *Gene Expr. Patterns* 4, 345–350.
- Uz, E., Alanay, Y., Aktas, D., Vargel, I., Gucer, S., Tuncbilek, G., von Eggeling, F., Yilmaz, E., Deren, O., Posorski, N., Ozdag, H., Liehr, T., Balci, S., Alikasifoglu, M., Wollnik, B., Akarsu, N.A., 2010. Disruption of ALX1 causes extreme microphthalmia and severe facial clefting: expanding the spectrum of autosomal-recessive ALX-related frontonasal dysplasia. *Am. J. Hum. Genet.* 86, 789–796.
- Varga, Z.M., Amores, A., Lewis, K.E., Yan, Y.L., Postlethwait, J.H., Eisen, J.S., Westerfield, M., 2001. Zebrafish smoothened functions in ventral neural tube specification and axon tract formation. *Development* 128, 3497–3509.
- Wada, N., Javidan, Y., Nelson, S., Carney, T.J., Kelsh, R.N., Schilling, T.F., 2005. Hedgehog signaling is required for cranial neural crest morphogenesis and chondrogenesis at the midline in the zebrafish skull. *Development* 132, 3977–3988.
- Wang, X., Lupo, G., He, R., Barsacchi, G., Harris, W.A., Liu, Y., 2015. Dorsoventral patterning of the Xenopus eye involves differential temporal changes in the response of optic stalk and retinal progenitors to Hh signalling. *Neural Dev.* 10, 7.
- Warr, N., Powles-Glover, N., Chappell, A., Robson, J., Norris, D., Arkell, R.M., 2008. Zic2-associated holoprosencephaly is caused by a transient defect in the organizer region during gastrulation. *Hum. Mol. Genet.* 17, 2986–2996.
- Wen, W., Pillai-Kastoori, L., Wilson, S.G., Morris, A.C., 2015. Sox4 regulates choroid fissure closure by limiting Hedgehog signaling during ocular morphogenesis. *Dev. Biol.* 399, 139–153.
- Westerfield, M., 1993. *The Zebrafish Book: A Guide for the Laboratory Use of Zebrafish (Brachydanio rerio)*. M. Westerfield, Eugene, OR.
- Williamson, K.A., FitzPatrick, D.R., 2014. The genetic architecture of microphthalmia, anophthalmia and coloboma. *Eur. J. Med. Genet.* 57, 369–380.
- Winata, C.L., Kondrychyn, I., Kumar, V., Srinivasan, K.G., Orlov, Y., Ravishankar, A., Prabhakar, S., Stanton, L.W., Korzh, V., Mathavan, S., 2013. Genome wide analysis reveals Zic3 interaction with distal regulatory elements of stage specific developmental genes in zebrafish. *PLoS Genet.* 9, e1003852.
- Wu, E., Vargevik, K., Slavotinek, A.M., 2007. Subtypes of frontonasal dysplasia are useful in determining clinical prognosis. *Am. J. Med. Genet. Part A* 143A, 3069–3078.
- Ybot-Gonzalez, P., Gaston-Massuet, C., Girdler, G., Klingensmith, J., Arkell, R., Greene, N.D., Copp, A.J., 2007. Neural plate morphogenesis during mouse neurulation is regulated by antagonism of Bmp signalling. *Development* 134, 3203–3211.
- Young, N.M., Chong, H.J., Hu, D., Hallgrímsson, B., Marcucio, R.S., 2010. Quantitative analyses link modulation of sonic hedgehog signaling to continuous variation in facial growth and shape. *Development* 137, 3405–3409.
- Zhao, L., Zevallós, S.E., Rizzoti, K., Jeong, Y., Lovell-Badge, R., Epstein, D.J., 2012. Disruption of SoxB1-dependent Sonic hedgehog expression in the hypothalamus causes septo-optic dysplasia. *Dev. Cell* 22, 585–596.
- Zhao, Q., Behringer, R.R., de Crombrughe, B., 1996. Prenatal folic acid treatment suppresses acrania and meroanencephaly in mice mutant for the Cart1 homeobox gene. *Nat. Genet.* 13, 275–283.